

Fluorescence Depolarization in Poly(*p*-phenylphenylenevinylene) and Related Oligomers

M. Hennecke* and T. Damerau†

Bundesanstalt für Materialforschung und -prüfung, Unter den Eichen 87, W-1000 Berlin 45, Germany

K. Müllen

Max-Planck-Institut für Polymerforschung, Ackermannweg 10, W-6500 Mainz 1, Germany

Received January 11, 1993; Revised Manuscript Received March 15, 1993

ABSTRACT: The photophysical behavior of poly(*p*-phenylphenylenevinylene) (PPPV) and several oligomeric model compounds in isotropic and anisotropic samples is investigated by means of polarized fluorescence spectroscopy. As long as excitation energy transfer and mutual alignment are considered, the behavior of PPPV can be modeled by a chain consisting of a distribution of independent oligomeric segments. The results of fluorescence polarization, e.g., the nonzero value of r in isotropic PPPV, cast doubt on the application of the semiconductor band model but favor an interpretation of spectroscopic properties in terms of molecular transitions. The orientation coefficients of the oligomers and of PPPV in stretched polyethylene are determined. The change of fluorescence spectra of oriented PPPV in stretched polyethylene demonstrates directly that conformational changes of the macromolecule influence the pathway of energy transfer.

Introduction

The optical properties of poly(*p*-phenylenevinylene) (PPV) have been studied extensively. It has been discussed whether optical transitions of this and other conjugated polymers are more adequately described by the semiconductor band model or alternatively by the exciton model.¹⁻⁶ It is in question as to what degree spectroscopic properties can be attributed to localized molecular transitions.

The generally accepted fact that the polymer chain consists of conjugated segments, separated from each other due to geometric distortions or chemical defects,^{4,5,7,8} favors the picture of molecular transitions in these polymer solids. As a consequence the behavior of PPV has often been discussed in comparison with oligomeric model compounds.⁹⁻¹²

By site-selective fluorescence spectroscopy Bässler and co-workers found strong evidence that the behavior of PPV and of its soluble derivative poly(*p*-phenylphenylenevinylene) (PPPV) is in disagreement with the band model.^{3,5,11} The properties of the polymers can be described by molecular spectroscopy in accordance to those of the oligomers. The conjugated segments can be described by a density of localized states (DOS), and excitation energy transfer (EET) within the DOS is observed.

In addition to site-selective spectroscopy, other fluorescence techniques have been used to investigate PPV.^{7,9,13-15} Polarized fluorescence experiments, instead of using unpolarized light, provide additional information on isotropic and anisotropic samples.^{1,4,5,16}

In isotropic specimens polarized excitation and emission spectra consist of spectral recording of the normalized total intensity I and of the degree of polarization r , given by the equations:

$$I = I_{VV} + 2I_{VH} \quad (1)$$

$$r = (I_{VV} - I_{VH}) / (I_{VV} + 2I_{VH}) \quad (2)$$

The indices V and H denote the vertical and horizontal

position of the polarizer in the excitation and the fluorescence beams, respectively. The intensities must be corrected for instrumental polarization sensitivity. In isotropic media r depends on the fundamental molecular anisotropy of the chromophore r_0 ($-0.2 \leq r_0 \leq 0.4$), the rotational mobility within fluorescence lifetime, and the orientational decorrelation by EET among the chromophores.

EET, as determined by the stationary or time-resolved measurement of the degree of fluorescence polarization, has been used as an observable for the structural properties of polymers and model compounds.¹⁷⁻²⁰

The main property of EET, which can be characterized by fluorescence polarization, is $G^a(t)$, the probability that the excitation resides at the site where it has been formed;²¹ in steady-state experiments $G^a(t)$ is Laplace transformed with the fluorescence lifetime to yield \tilde{g}^a .

Theoretical treatments are given for isoenergetic chromophores that may have a nonrandom positional distribution (e.g., chromophores attached to a polymer chain)^{17,18} or for a two-energy site system.²² Recently a calculation of $G^a(t)$ for a distribution of site energies has been published.²³

Usually it is assumed that the mutual orientation of the chromophores is not correlated; i.e., chromophores that are populated by EET show, on the average, no fluorescence polarization ($r = 0$).^{24,25} Only a few authors consider orientational correlation in their theories.^{26,27}

The situation in PPPV is a combination of both aspects: First, one has to take into account a distribution of conjugated segments and site energies. Second, an orientational correlation of the segments has to be considered not only in crystallites but also in amorphous regions because of the stiffness of the chain.

For a qualitative discussion of EET in this system, the following rough approximation is used:

$$r = r_0[\tilde{g}^a + (1 - \tilde{g}^a)\langle^2P_2\rangle] \quad (3)$$

$\langle^2P_2\rangle$ ($0 \leq \langle^2P_2\rangle \leq 1$) is a second-order pair orientational order coefficient of a pair-type distribution function, taken in the spatial range of EET. In perfectly isotropic solids, where even neighbored sites are uncorrelated, $\langle^2P_2\rangle = 0$. Formula 3 is deduced from Weber's law of additive

* Present address: Institut für Physikalische Chemie der TU Clausthal, Arnold-Sommerfeld-Strasse 4, W-3392 Clausthal-Zellerfeld, Germany.

Table I. Experimental Results for Compounds 1a-c, 2a,b and 3 Incorporated in Isotropic and Anisotropic Films^a

compd	$\lambda_{ex}/\lambda_{em}$ (nm)	r_0 (PS)	r (PE)	model A		model B ($\epsilon = \text{random}$)			
				$\langle P_2 \rangle$	$\langle P_4 \rangle$	$\langle P_2 \rangle$	$\langle P_4 \rangle$	α	α'
1a	360/420	0.35	0.27	0.19	-0.10	0.18	-0.10	9.5	14.0
1b	390/460	0.35	0.27	0.36	-0.05	0.32	-0.02	9.5	14.0
1c	405/480	0.35	0.27	0.54	0.08	0.51	0.09	11.1	12.8
2a	360/420	0.35	0.27	0.55	0.07	0.54	0.07	8.0	14.9
2b	360/420	0.35	0.27	0.33	-0.03	0.32	-0.02	10.7	13.1
3	400/480	0.18	0.22	0.35	0.01	0.32	0.02	24.5	24.6

^a r_0 is determined from an isotropic PS film and used to calculate the orientation coefficients for the oligomers. r is determined from an unstretched PE film. $\langle P_2 \rangle$ and $\langle P_4 \rangle$ are calculated from the various polarized components of a PE film, stretched to 200% of the initial length, according to models A and B. Each pair of orientation coefficients of model A is the average of eight different combinations to determine F_{ZY}/F_{ZZ} and F_{YV}/F_{ZY} .

polarization²⁸ by dividing the emitting chromophores into two groups: those that were initially excited ($r = r_0$) and those that are excited by EET ($r = r_0 \langle {}^2P_2 \rangle$). Equation 3 may be applied to multichromophore systems if r_0 has the same value for all chromophores.

By preparing systems with various orientational order and a different density of fluorophores, the range and dimension of EET can be varied and it is possible to discuss r with respect to \bar{g}^a and $\langle {}^2P_2 \rangle$.

In anisotropic systems, polarized fluorescence measurements yield information about the orientation distribution function (odf) and the transition moment direction of the oriented fluorescent molecules.²⁹ The transition moment direction is of fundamental interest when using polarized light. In order to evaluate the orientation coefficients that characterize the odf, one needs information about both the symmetry and the photophysical behavior of the chromophores and the macroscopic symmetry of the specimen.²⁹⁻³¹

Stretched films of polyethylene, frequently used as anisotropic host media, show uniaxial symmetry around the stretching direction Z .²⁹ If the incorporated chromophores have the shape of long thin molecules, the long axis can be assumed to be the unique axis of orientation (geometric rotational symmetry).

The photophysical behavior of the chromophores is in general described by the molecular tensors of absorption $A = (a_{ij})$ and emission $E = (e_{ij})$ (i and j are the coordinates x, y, z of the molecular framework).^{29,32}

In the most simple case A and E are diagonal tensors in the same molecular framework, wherein z is the unique axis, and the anisotropy of the diagonalized tensors is the same:³²

$$p = \frac{2a_{yy}}{2a_{yy} + a_{zz}} = \frac{2e_{yy}}{2e_{yy} + e_{zz}} \quad (4)$$

In general the geometric unique axis does not need to coincide with one axis of the diagonalized tensor.

p is related to the experimentally determined anisotropy (cf. eq 2) by

$$r_0 = (2 - 3p)^2/10 \quad (5)$$

With the knowledge of r_0 , two orientation coefficients $\langle P_2 \rangle$ and $\langle P_4 \rangle$ are determined by two ratios F_{ZY}/F_{ZZ} and F_{YV}/F_{ZY} from the components of the fluorescence tensor F_{UV} (U and V are the coordinates X, Y, Z of the macroscopic framework). The formulas are given elsewhere.^{31,33} This method of evaluation is called model A in Table I.

The transition moment directions (i.e., the main axes of the optical tensor) for molecules belonging to point groups of high symmetry (e.g., C_{2v} or D_n) are restricted to the geometric directions of symmetry.²⁹ Assuming that the geometric long axis of the molecule tends to orientate toward the stretching direction, the sign of $\langle P_2 \rangle$ already

indicates whether the z -axis of the tensor is directed along the long molecular axis or perpendicular to it.

In molecules of low symmetry like C_{2h} , transition moments are restricted to the mirror plane only and might form any angle with the long molecular axis.²⁹ In this case the sign of $\langle P_2 \rangle$, calculated by the method above, only indicates whether the transition moment forms an angle greater or smaller than 54.7° (magic angle) with the long axis.

In order to attribute the transition moment direction in low-symmetry molecules more precisely, we used an alternative method to evaluate $\langle P_2 \rangle$ and $\langle P_4 \rangle$, outlined by Nobbs et al.³⁰

Absorption and emission are described by distinct transition moment vectors forming different angles with the unique axis of the molecule, α and α' , respectively. In this model the emission anisotropy is determined by the angle α'' between the absorption and emission moment according to

$$r_0 = 0.2(3 \cos^2 \alpha'' - 1) \quad (6)$$

Additionally the difference ϵ between the azimuthal angles of emission and absorption has to be considered. By an approximation procedure one obtains $\langle P_2 \rangle$, $\langle P_4 \rangle$, α , and α' , if an assumption for ϵ has been made; e.g., ϵ is chosen to be π or random (model B in Table I). This model accounts for the difference between F_{ZY} and F_{YZ} , whereas $F_{ZY} = F_{YZ}$ is implied by the first evaluation procedure. Careful interpretation is necessary, since differences between F_{ZY} and F_{YZ} may be caused by various effects during measurement.

It should be noted that, in the case of $\cos^2 \alpha = \cos^2 \alpha'$ and random ϵ , both methods are identical.³¹

Experimental Part

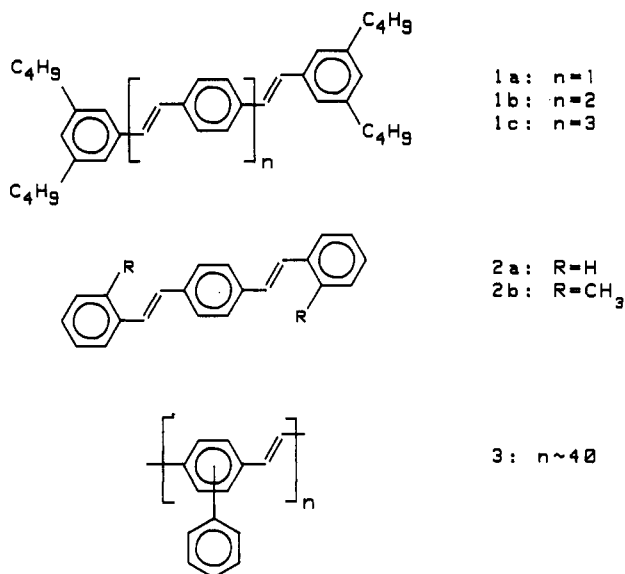
Materials under investigation are poly(*p*-phenylphenylenevinylene) (PPPV; 3) and various oligomeric model compounds (1a-c and 2a,b).

The oligomers 1a-c are prepared by sequences of Wittig reactions³⁴ and exhibit all-trans configuration. *tert*-Butyl groups are attached to the terminal phenyl rings to improve solubility. The oligomers form a series with $n = 1, 2$, and 3 repetitive units plus the terminal phenyl rings. 1,4-Distyrylbenzene (2a) is supplied by H. Meier, Mainz, Germany, and 1,4-bis(2-methylstyryl)benzene (2b) is commercially available (Riedel-de-Haen).

PPPV (3), a soluble derivative of the insoluble PPV, is synthesized via a Heck reaction³⁵ and is supplied from A. Greiner, Marburg, Germany. The molecular weight is $M_w = 7000$.

Fluorescence experiments are carried out on a commercial spectrometer (Spex-Fluorolog) with an angle of 90° between the excitation and fluorescence beams. The polarization equipment consists of two Glan-Thompson rotatable prism polarizers (Hanle, Berlin, Germany).

For the measurements of fluorescence polarization, the chromophores are incorporated into films of polystyrene or polyethylene in order to avoid rotational mobility within the



fluorescence lifetime. Isotropic films are placed between the hypotenuse plane of two 30–60–90° prisms, with glycerol as an immersion liquid. Anisotropic films are placed between glass plates in an in-house-built device and are rotated around the normal axis X of the film plane in order to determine the exact horizontal and vertical position of the stretching direction Z (Figure 1). These positions are free from birefringence and are used to calculate $\langle P_2 \rangle$ and $\langle P_4 \rangle$.

Polystyrene films (PS) are cast from solutions in tetrahydrofuran (THF) to a thickness of 130 μm . The chromophore to polystyrene weight ratio of the dilute films was $1/10^4$ or $1/10^6$; in this concentration range no significant variation in the spectra or the degree of polarization was observed. Thin films of about 1 μm are produced by spin coating on a glass plate, either from a solution with polystyrene (weight ratio PPPV/polystyrene: $1/10^4$ and $1/5$) or from a pure PPPV solution.

Blown films of low-density polyethylene (Lupolene, BASF; 40 μm) are doped with the chromophores from solutions in toluene (1a–c and 2b) or chloroform (2a and 3). The concentration of the solutions is 10^{-3} mol/L for 2a and 2b, 10^{-4} mol/L for 1a–c, and 1.5 g/L for 3. After a diffusion time of 48 h for each sample, they are washed with the corresponding solvent and dried. The actual concentration of the chromophore in the film is not known and especially for PPPV (3) it is doubtful if the macromolecules are homogeneously distributed or are adsorbed at the surface, but this is not important for a qualitative discussion. Strips, 15 mm wide, are stretched from the initial length of 20 mm to 60 mm at a rate of 0.1%/s. The films are taken from the stretching machine and allowed to relax a few minutes, before determining $\langle P_2 \rangle$ and $\langle P_4 \rangle$.

In the experimental arrangement of Figure 1 the measured fluorescence intensities are related to the components of the fluorescence tensor F_{UV} by the following equations:³⁶

$$I_{VVV} = KF_{ZZ} \quad (7a)$$

$$I_{VVH} = KF_{ZY} \quad (7b)$$

$$I_{VHV} = KF_{YZ} \quad (7c)$$

$$I_{VHH} = K[\cos^2(\theta_E + \theta_F)F_{YY} + \sin^2(\theta_E + \theta_F)F_{YX}] \quad (7d)$$

$$I_{HVV} = KF_{YY} \quad (7e)$$

$$I_{HVH} = K[\cos^2 \theta_F F_{YZ} + \sin^2 \theta_F F_{YX}] \quad (7f)$$

$$I_{HHV} = K[\sin^2 \theta_E F_{YX} + \cos^2 \theta_E F_{ZY}] \quad (7g)$$

The subscripts of I denote the positions of the stretching direction, the excitation polarizer, and the emission polarizer, respectively. θ_E is the angle between the excitation beam inside the film and the normal of the film plane (governed by the angle of incidence ($\beta_0 = 60^\circ$) and Snell's law). θ_F is the corresponding angle for the fluorescence beam. The instrumental constant K is not important for calculations.

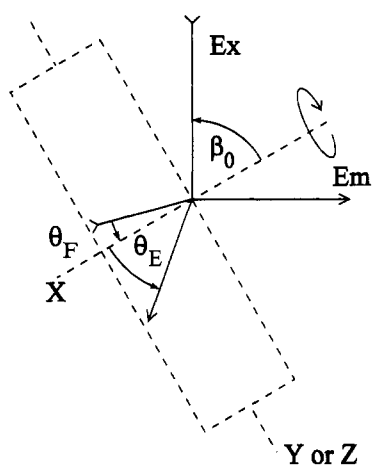


Figure 1. Geometry of the polarized fluorescence experiment of a stretched film in a spectrometer with a 90° angle between the excitation and emission beams. A framework XYZ is attached to the specimen. The axis X of rotation is normal to the film plane. To avoid birefringence, the stretching direction Z must be aligned normal to the paper plane (vertical position) or within this plane (horizontal position). θ_E and θ_F depend on the angle of incidence β_0 and Snell's law.

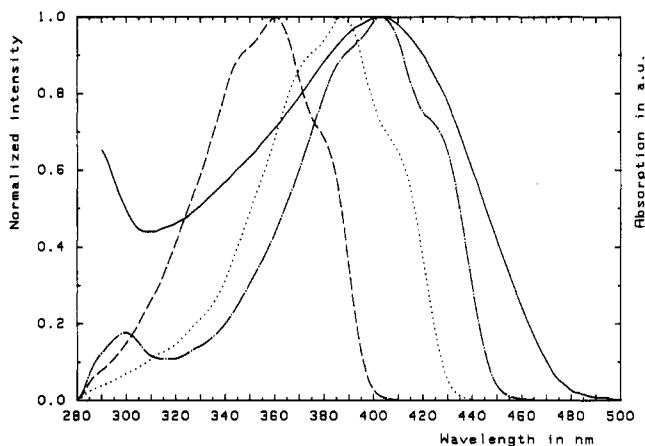


Figure 2. Normalized excitation spectra of the oligomers 1a (---, $\lambda_{em} = 420$ nm), 1b (···, $\lambda_{em} = 455$ nm), and 1c (- · - ·, $\lambda_{em} = 477$ nm) in toluene, 1×10^{-6} mol/L (left-hand scale). Slit-width excitation/emission: 1.8/1.8 nm. Absorption spectrum of PPPV (3) in toluene (—), 1×10^{-3} g/L, maximum OD = 0.17 at 405 nm (right-hand scale).

The most reliable way to calculate the two ratios mentioned above was found to be as follows: F_{ZY}/F_{ZZ} is obtained by dividing (7a) and (7b) and F_{YY}/F_{ZY} by evaluating $F_{ZY} = F_{YZ}$ from (7f) and (7g) and combining it with (7e). The total fluorescence intensity often may vary for the various positions of the stretching direction, and this is circumvented by taking ratios from intensities of the same rotational position.

For the second method of evaluation one has no alternative to compare F_{YY} from the horizontal position of the stretching direction with other intensities measured at the vertical position. Therefore, some differences in $\langle P_2 \rangle$ and $\langle P_4 \rangle$ values of the two models A and B may be due to different absolute intensities at the two particular director positions.

Results and Discussion

1. Isotropic Samples. 1.1. Oligomeric Model Compounds. The fluorescence excitation spectra of the oligomers 1a–c in toluene solution are shown in Figure 2. They coincide with the UV/vis absorption spectra. The energy of the $S_0 \rightarrow S_1$ transition decreases with increasing extension of the conjugated system, but the spectral shape does not change; the maxima are 360, 387, and 403 nm for $n = 1, 2, 3$. Due to solvent interaction the excitation spectra

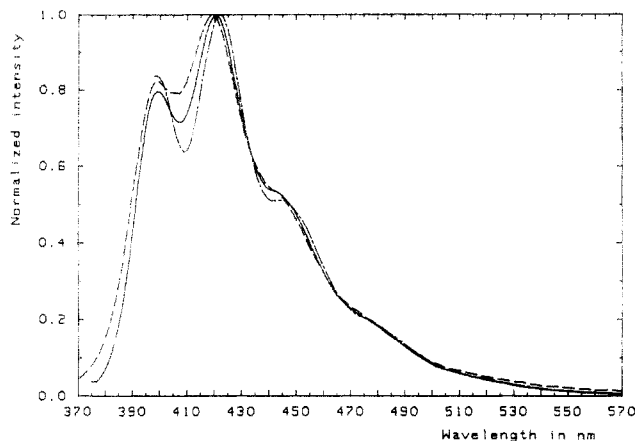


Figure 3. Emission spectra at various excitation wavelengths of oligomer 1a in a polystyrene film of 100 μm (weight ratio: 1/10⁴): $\lambda_{\text{ex}} = 310$ nm (---), $\lambda_{\text{ex}} = 363$ nm (—), $\lambda_{\text{ex}} = 390$ nm (-·-). Slit width: 1.8/1.0 nm.

in the polystyrene film are red shifted by 4 nm. The maximum for the $S_0 \rightarrow S_1$ transition of the oligomers with $n = 4, 5,$ and $6,$ as determined by UV/vis absorption in chloroform solution, increases only slightly to 417.9 nm with a maximum at $n = 5.$ ³⁴ In view of the behavior of the oligomeric compounds, the maximum absorption for PPPV should lie around 415 nm or at shorter wavelength.

Fluorescence spectra of the oligomers 1a–c in toluene are also very similar to each other (e.g., Figure 3 for 1a), and they show a Stoke shift of 2300 cm^{-1} between the excitation maximum and the first emission peak. In low-viscosity solvents no dependence of the fluorescence spectrum upon variation of λ_{ex} has been observed, indicating that the fluorescence transition is not influenced by selective photoexcitation of rotamers. For 1a and 2a this fact has already been reported.^{37,38}

In polystyrene films the excitation and, more pronounced, the emission spectra show dependence on λ_{em} and λ_{ex} , respectively. In the emission spectrum of oligomer 1a, for example, the minimum between the two peaks becomes deeper the larger the chosen excitation wavelength is; a slight shift in the maximum position is also observed (Figure 3). This behavior is obviously viscosity induced, as has been pointed out by Castel and Fischer for several 1,2-diarylethylenes.³⁹ The S_0 and S_1 states have their potential energy minima at different combinations of twisting angles around the C–C and C=C bonds. As the viscosity increases, emission from unrelaxed S_1 states becomes important, leading to the observed variations.

In polystyrene films no rotational depolarization within the fluorescence lifetime and no EET occurs ($g_s = 1$); i.e. $r = r_0$ is measured in dilute films. All oligomers show the same behavior with respect to r : The value of r remains constant throughout the $S_0 \rightarrow S_1$ transition excitation and emission bands and is about $r_0 = 0.35 \pm 0.01$, indicating a strong anisotropy of the molecular absorption and emission tensor (Figure 4).

At higher concentrations in general r is lowered. As an example the emission spectrum of oligomer 1c in polystyrene (weight ratio: 1/115) is shown in Figure 4. The decrease of r is not uniform throughout the spectrum, since a significant increase of r occurs in the short-wavelength part. Some effects have to be considered. First, EET prior to emission leads to a general decrease of r . Second, in samples with a high optical density trivial reabsorption and reemission causes a decrease of r ,^{28,40–42} which need not be uniform. Third, it is known that aromatic compounds easily form aggregates in solid solution, which may have other fluorescence properties.

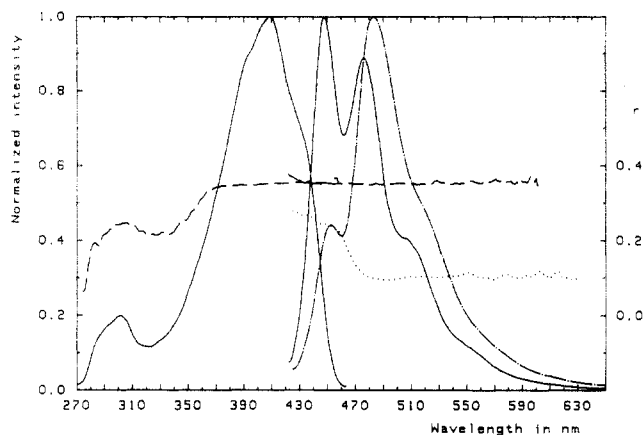


Figure 4. Polarized spectra (see (1) and (2)) of oligomer 1c in polystyrene films of 130- μm thickness. Excitation ($\lambda_{\text{em}} = 478$ nm) and emission ($\lambda_{\text{ex}} = 405$ nm) spectra at a weight ratio of 1/10⁶ (—, $I_{\text{VV}} + 2I_{\text{VH}}$, left-hand scale) and corresponding degree of polarization (---, right-hand scale). Slit width: 2.2/2.7 nm. Emission spectrum ($\lambda_{\text{ex}} = 405$ nm) at a weight ratio of 1/115 (-·-) and corresponding degree of polarization (· · ·). Slit width: 1.8/0.9 nm.

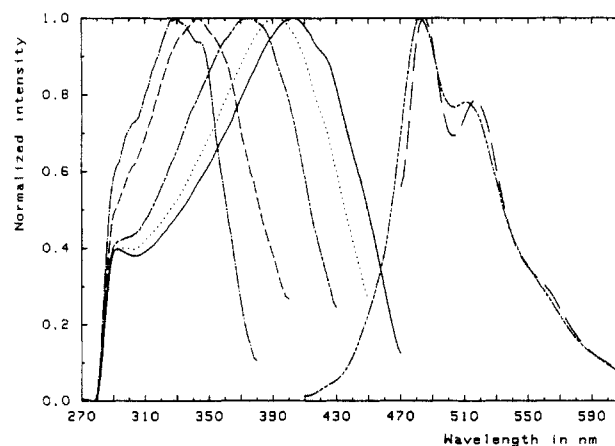


Figure 5. Excitation and emission spectra of PPPV (3) in toluene (1×10^{-3} g/L) at various emission and excitation wavelengths: $\lambda_{\text{em}} = 390$ nm (---), $\lambda_{\text{em}} = 410$ nm (---), $\lambda_{\text{em}} = 440$ nm (---), $\lambda_{\text{em}} = 460$ nm (· · ·), $\lambda_{\text{em}} = 480$ nm (—), $\lambda_{\text{ex}} = 400$ nm (---), $\lambda_{\text{ex}} = 460$ nm (—). Slit width: 2.2/2.2 nm.

At high concentration the spectra (especially the excitation spectra) are distorted due to reabsorption.

1.2. Poly(*p*-phenylphenylenevinylene). The long-wavelength part of the UV/vis absorption spectrum of PPPV in THF or toluene (Figure 2) is a broad structureless band beginning at 485 nm, peaking at 400 nm, and having a full width at half-maximum of 7500 cm^{-1} . The peak position is similar to that of oligomer 1c, but the spectrum is significantly broader, probably due to a distribution of segments of various conjugation length.

In the case of the oligomers the fluorescence excitation spectrum coincides with the absorption spectrum, but for PPPV it depends significantly on the wavelength of emission, in particular for $\lambda_{\text{em}} < 480$ nm (Figure 5). On the other hand, the emission spectrum depends only slightly on the excitation wavelength in such a way that the peak to the red of the maximum becomes more pronounced at a long excitation wavelength. This different behavior of excitation and fluorescence spectra cannot be explained by photoselective excitation of various rotamers, which would require a significant variation of emission spectra too. The behavior is observed in fluid as well as in solid solutions; i.e., a viscosity-induced effect can also be excluded.

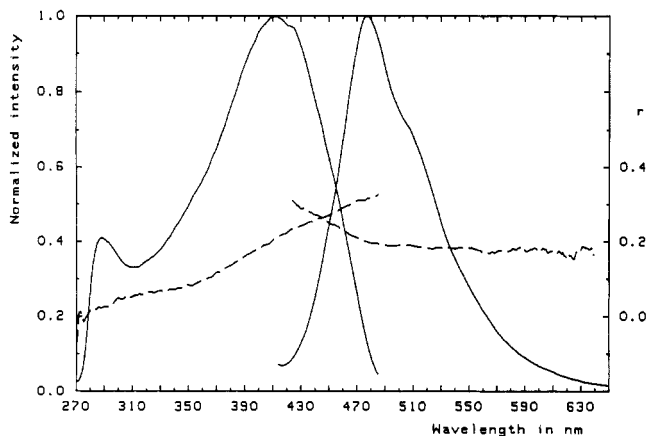


Figure 6. Polarized excitation ($\lambda_{em} = 510$ nm) and emission spectrum ($\lambda_{ex} = 400$ nm) of PPPV in polystyrene film (130 μm) at a weight ratio of $1/10^5$ (—, $I_{VV} + 2I_{VH}$, left-hand scale) and corresponding degree of polarization (· · ·, right-hand scale). Slit width: 2.7/3.6 nm.

The results can easily be explained by rapid and efficient EET from the absorbing segment (the length depending upon λ_{ex}) to the longest and therefore energetically lowest segment on each chain prior to emission. Regarding the whole sample, the emitting segments from each chain form a narrow distribution of conjugation lengths, leading to the narrow emission spectrum peaking at 480 nm. Upon selecting short wavelengths for the emission (e.g., $\lambda_{em} = 450$ nm), one monitors preferentially a subset of chains with shorter length of emitting segments, leading to the observed shift in the excitation spectrum. The effect vanishes when interchain EET becomes significant, e.g., in concentrated solutions (see below).

For PPPV the degree of polarization increases with increasing wavelength in the excitation spectrum, as shown in Figure 6 for a dilute solution in PS. At $\lambda_{em} = 510$ nm it is about $r = 0.05$ for $\lambda_{ex} = 310$ nm and increases to $r = 0.32$ for $\lambda_{ex} = 480$ nm, which is similar to the constant value of the oligomers.

Bässler and co-workers^{3,5} considered PPPV and PPV as random organic solids with an energy distribution of localized sites, subject to random walk of an excitation. The sites are attributed to segments of the polymer chain with a few monomer units only. Dispersive EET, usually observed at low temperature, but in polymers also at elevated temperatures,^{20,23} will occur, and as a consequence the range of transfer (and its observable r) is dependent upon the excitation wavelength. According to (3), r will increase with increasing wavelength due to an increase of \bar{g}^a .

Generally one has to accept that $\langle {}^2P_2 \rangle$ (see (3)) is a function of the range of EET (i.e., \bar{g}^a): $\langle {}^2P_2 \rangle$ approaches its bulk value as \bar{g}^a decreases. If the EET is confined to a small number of sites, the discussion can only be qualitative. r is found to be nonzero, even for small λ_{ex} , e.g., 310 nm, where short segments absorb and transfer the excitation to sites of lower energy. r and therefore \bar{g}^a depend on λ_{ex} , i.e., on the relative absorption probability of the emitting site. Therefore, a value of $r > r_0 \bar{g}^a$ indicates mutual alignment of segments in the distance range of EET; perfect alignment, i.e., $\langle {}^2P_2 \rangle = 1$, requires $r = r_0$ which is in contradiction to the observed wavelength dependence. From Figure 6 we conclude that $\langle {}^2P_2 \rangle$ is small but nonzero in dilute PPPV solution.

The fluorescence emission spectrum of PPPV shows two significant points in comparison with oligomer 1c (Figures 4 and 6): First, the degree of polarization, which has a constant value of $r = 0.18$ in the major part of the

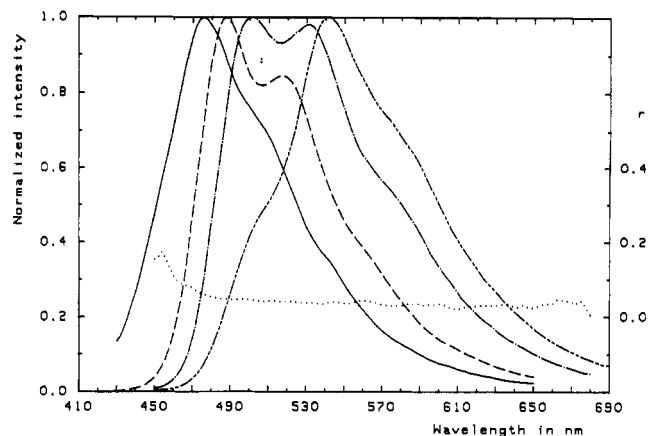


Figure 7. Emission spectra of PPPV in various films (left-hand scale): weight ratio 1/10 000 in polystyrene (—, $\lambda_{ex} = 400$ nm, thickness about 1 μm); 1/5 in polystyrene (---, $\lambda_{ex} = 400$ nm, thickness about 1 μm); pure thin film (- · - ·, $\lambda_{ex} = 400$ nm, thickness about 0.2 μm , OD = 0.20 at 407 nm); pure thick film (· · ·, $\lambda_{ex} = 420$ nm, thickness about 15 μm). The degree of polarization of the pure thin film is also shown (· · ·, right-hand scale). The slit widths are 4.5/5.4, 1.8/1.5, 0.9/3.0, and 0.9/3.0 nm, respectively.

emission spectrum, increases in the short wavelength region and, second, the short-wavelength peak is absent in PPPV.

We explain the increase of r by various emitting species responsible for the fluorescence spectrum, as has been shown above by the dependence of the excitation spectrum upon λ_{em} . The short segments, emitting preferentially in the short-wavelength part, show a higher degree of polarization than the longer segments that are populated by EET.

Although the PPPV spectrum in Figure 6 is that of a dilute solution (weight ratio PPPV/polystyrene: $1/10^5$), one may also explain the increase of r by the same arguments as in case of the concentrated oligomer film in Figure 4. A high chromophore density, needed for this interpretation, may result from two facts. PPPV is in general immiscible with polystyrene.⁴³ Aggregates may be formed during film casting, leading to a higher local concentration. Furthermore, at sufficient molar mass the polymer chain itself carries a high chromophore density.

The absence of the short-wavelength peak in the emission spectrum of PPPV (Figure 6) is worth mentioning. Not only the oligomers (Figure 4) but also all spectra of PPV films reported in the literature (e.g., refs 1, 4, 5, 13, and 16) show three spectral features (maximum and two local maxima or shoulders); some spectra of PPPV recorded at low temperature show these features too.^{3,12} The discrepancy can be clarified by preparing films of PPPV in PS of higher concentration and films of pure PPPV. When dealing with cast films, 130 μm thick and of weight ratios greater than 1/1000, the spectra are distorted by reabsorption effects. Therefore, we used thin spin-coated films on quartz glass; in very thin films reabsorption is negligible.^{28,40,41,44}

Figure 7 compares the emission spectra of PPPV in PS (weight ratios: 1/10000 and 1/5, 1 μm thick) and of two pure PPPV films. The spin-coated thin film has an optical density (OD) of 0.20 at 407 nm (thickness about 0.2 μm); the solution-cast thick film (about 15 μm) is turbid and depolarizes the light.

It has to be noted that pure films show photoreactivity under usual conditions in the spectrometer, documented by a significant decrease of the absolute fluorescence intensity. For example, during 100 min of illumination at $\lambda_{ex} = 370$ nm (slit width: 3.5 nm) $1/2$ of the intensity is

lost. Spectra of pure films in Figure 7 were recorded at a slit width of 0.9 nm, and the intensity does not decrease by more than 10% during the measurement; changes in the spectra are negligible for the following discussion. A paper on the photoreactivity of PPPV will be published separately.

Except for the thick PPPV film the excitation spectra of the films (not shown) are not distorted by reabsorption. Therefore, this trivial effect is not responsible for the obvious shift of the maxima in the emission spectra of the 1/10 000, the 1/5, and the pure thin film in Figure 7. The shift between the 1/10 000 and the 1/5 film is caused by interchain EET enabled in the latter by increased chromophore concentration. With interchain EET the excitation is not restricted to the chain where it has been created but it can migrate to the energetically favored segments of the whole sample, leading to a red shift of fluorescence. In concentrated films, like the 1/5 one, the distribution of fluorescing segments is narrower than that in dilute solution, because short segments do not contribute. Additional support for this interpretation comes from the fact that the significant dependence of the excitation spectra on the emission wavelength (cf. Figure 5) vanishes gradually from the 1/10 000 to the 1/5 film.

The red shift in the emission spectrum of the pure film in comparison with the 1/5 film may be caused by an even stronger influence of the effect outlined above. Furthermore, the matrix change from PS to PPPV may have a solvatochromic effect.

The dependence of the fluorescence on the film thickness was also verified; the considerable difference between the thick and the thin pure film is simply due to reabsorption. The emission maximum of the thin film vanishes and only appears as a shoulder. As a result, the fluorescence of the thick film shows shoulders at both sides of the maximum; this spectral structure is also observed in the published PPV spectra.^{1,4,5,13,16}

The PPPV spectra in Figure 7 should be compared to the polarized spectra of PPV films that have already been published.^{5,16} The excitation spectra are difficult to compare, because they are distorted at high optical densities. The emission spectrum of PPV peaks at 555 nm, while the pure thick PPPV film has its maximum at 542 nm. It has been argued that the effective conjugation length in PPV is larger, because the phenyl substituents impose steric hindrance in PPPV.¹² Our result may be a confirmation of the statement, but one has to be very careful: the PPPV fluorescence spectra are more sensitive to sample preparation (i.e., concentration, thickness, and optical density) than PPV.

The degree of polarization has also been shown to depend on sample preparation but is nonzero throughout the excitation and emission spectra for PPV and PPPV. This is in contrast to the behavior of conventional aromatic polymers. Since it has been proved that three-dimensional EET occurs in PPV,⁵ a nonzero value of r is only possible (provided that quenching processes are absent), if $\langle {}^2P_2 \rangle$ takes a considerable value (cf. (3)). The comparison of the course of r in a 50-nm PPV film¹⁶ and in a thin PPPV film (Figure 7) shows more depolarization in the case of PPPV. Since r_0 and g^* are similar for both polymers, the molecular alignment in PPPV, as indicated by $\langle {}^2P_2 \rangle$, must be lower due to the phenyl substituents.

2. Anisotropic Samples. The orientation coefficients $\langle P_2 \rangle$ calculated for an unstretched film show values between -0.01 and 0.03 for all compounds **1a-c**, **2a,b**, and **3**, which indicate a nearly isotropic distribution of the

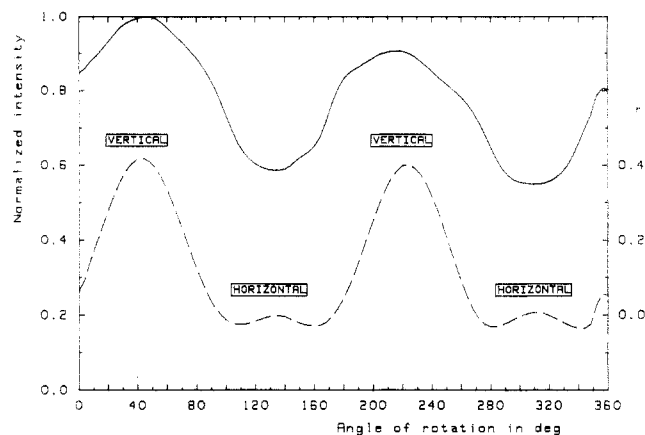


Figure 8. Fluorescence intensity $I_{VV} + 2I_{VH}$ (—, left-hand scale) and degree of polarization r (---, right-hand scale) during rotation around the normal axis to the plane of a polyethylene film doped with PPPV and stretched to 200% of the initial length ($\lambda_{ex} = 400$ nm, $\lambda_{em} = 480$ nm). The positions of the stretching direction are indicated (slit width: 5.4/5.4 nm).

chromophores in the amorphous regions of the polymer, in spite of the small birefringence of about $\Delta n = 3 \times 10^{-3}$.

In comparison with r_0 in the polystyrene matrix, the values of the oligomers (cf. Table 1) are lowered in unstretched polyethylene ($r = 0.27$), which may be due to rotational or matrix depolarization effects in the semicrystalline polymer. It was shown earlier^{47,48} that during stretching these sources of depolarization vanish; therefore, r_0 was used for the evaluation of the orientation coefficients. For PPPV r is slightly larger in an unstretched polyethylene matrix ($r = 0.22$ at $\lambda_{ex} = 400$ nm, $\lambda_{em} = 480$ nm) than in PS ($r = 0.18$); the first value is used for calculations.

The experimental result for the rotation of a stretched polyethylene film doped with PPPV (birefringence $\Delta n = 0.027$) is shown in Figure 8. In an anisotropic sample the plotted intensity $I_{VV} + 2I_{VH}$ does, of course, not represent the total fluorescence intensity, which cannot be calculated during rotation. In Figure 8 the value of r is not constant during rotation (as in the isotropic case), but it increases for the vertical position of the stretching direction and decreases for the horizontal one; this is indicative of a positive value of $\langle P_2 \rangle$. The results are listed in Table I for models A and B.

Model B takes into account more experimental data and allows a more detailed characterization of the chromophore, especially concerning the angle ϵ (see above). The procedure of evaluation yields no solution for $\epsilon = 0$. Taking $\epsilon = \pi$ leads to orientation coefficients that are lower than those for taking ϵ as random; this was observed for all chromophores (e.g., for oligomer **1c**, $\epsilon = \pi$ yields $\langle P_2 \rangle = 0.50$ and $\epsilon = \text{random}$ $\langle P_2 \rangle = 0.51$). Nobbs et al.³⁰ found that the choice $\epsilon = \text{random}$ is the most appropriate for the compound 4,4'-bis(benzoxazolyl)stilbene, which is similar to the chromophores used here.

For all compounds except oligomer **2a** (1,4-distyrylbenzene), the obtained intensities F_{ZY} and F_{YZ} differ up to 5% from each other, usually $F_{ZY} > F_{YZ}$. Only for oligomer **2a** was the difference about 10%. Therefore, the angles α and α' differ only by a few degrees (Table 1) ($\alpha = \alpha'$ for $F_{ZY} = F_{YZ}$). Consequently, model B yields results similar to model A, where $F_{ZY} = F_{YZ}$ is assumed.

This leads to a conclusion that could not be drawn from model A alone: In model A $\langle P_2 \rangle$ is the orientation coefficient of the main optical tensor axis of the molecule, while in model B $\langle P_2 \rangle$ refers to the orientation of the geometrically unique axis of the molecule. The coincidence of the results of both models indicates that the physical

behavior of the chromophores can be described by absorption and emission tensors with their main axis along the unique molecular axis.

Furthermore, it is obvious that the orientation coefficients of the various molecules in Table 1 are due to different degrees of alignment of the molecules and are not due to different photophysical properties.

The $\langle P_2 \rangle$ and $\langle P_4 \rangle$ parameters of the chromophores vary significantly with the geometrical shape of the molecules. $\langle P_2 \rangle$ of oligomers 1a-c increases, because the length and the ratio of length to thickness is increased. Comparing 1a and 2a, having the same length of the conjugated system, demonstrates the dramatic effect of the *tert*-butyl groups on the orientation of 1a. Likewise CH_3 groups, comparing 2a and 2b, influence the process of orientation. The macromolecule PPPV, as probed by its finally emitting segment, shows a significant degree of orientation, which is on the order of magnitude of oligomer 1b. This requires orientation of the whole polymer chain. Hagler et al. find significantly higher degrees of orientation for the stretched specimen of another derivative of PPV blended with polyethylene.^{49,50}

The values of $\langle P_4 \rangle$ are within the physically allowed limits with respect to $\langle P_2 \rangle$. But $\langle P_4 \rangle$ is very sensitive to the chosen value of r_0 and carries a large experimental error. Nevertheless, $\langle P_4 \rangle$ is related to $\langle P_2 \rangle$ in such a way that $\langle P_4 \rangle$ is greater the higher the degree of orientation is.

It is worth questioning whether PPPV, having a degree of polymerization of about 40, maintains its conformation during stretching (as is expected for the oligomers) or whether it undergoes conformational changes like a flexible polymer. In the first case emission spectra should be independent of the stretching ratio. Possible conformational changes are rotations around C-C single bonds of the vinylene units or around single bonds at chemical defects. The first change would influence the effective conjugation length and the second the pathway of EET between the segments.

The spectra of the stretched polyethylene films doped with PPPV can be recorded for various polarized components, e.g., setting the excitation and emission polarizers to the vertical position and the stretching direction vertical (I_{VVV}) or horizontal (I_{HVV}) (Figure 9). In the unstretched state the corresponding spectra are nearly identical.

The process of orientation of the chain as a whole (e.g., rotation of the macromolecule) will not alter the energetic distribution of the chromophoric segments. Therefore, if EET is complete, the normalized emission spectra of all polarized components will be identical. This may not be true for the excitation spectra, because the relative absorption probability of certain segments may be changed by orientation. Hence, differences in the emission spectra of polarized components notify changes of the energetic distribution of emitting segments, caused by conformational changes during stretching. Consequently such differences were not found in the case of oligomers 2a and 2b.

In PPPV a slight, but reproducible, effect is observed: In comparison with the normalized emission spectrum of an unstretched film and with the spectrum of I_{HVV} of a stretched one, the component I_{VVV} shows less intensity at wavelengths above 500 nm; i.e., the energetic distribution of fluorescent segments is shifted to higher energies (Figure 9). In view of the low concentration of PPPV in the polyethylene film, it was verified carefully that fluorescence impurities of polyethylene do not affect the results. Hagler et al.^{49,50} use other experimental conditions, but

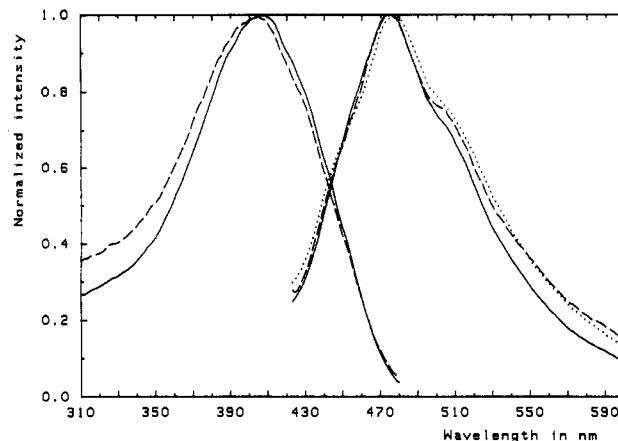
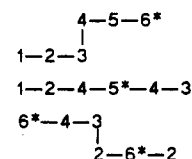
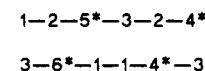


Figure 9. Normalized excitation ($\lambda_{em} = 500$ nm) and emission spectra ($\lambda_{ex} = 400$ nm) of a polyethylene film doped with PPPV, stretched to 200% of the initial length, for the vertical and horizontal positions of the stretching direction and with both polarizers in the vertical position (slit width: 5.4/5.4 nm). The spectra represent the components F_{ZZ} (I_{VVV} , —) and F_{YY} (I_{HVV} , - - -) of the fluorescence tensor (cf. (7a) and (7e)). The ratio of the absolute intensities at $\lambda_{ex} = 400$ nm/ $\lambda_{em} = 475$ nm is about $I_{VVV}/I_{HVV} = 3$. The emission spectrum of the unstretched film is also shown (\cdots); the corresponding excitation spectrum (not shown) is similar to I_{HVV} .

A: Any absorption will finally excite the longest segment of the chain by EET.



B: An excitation can also be trapped at a segment, which has not the longest conjugation length.



C: Same joined sequence as B, but conformational folding allows non-neighboured EET, leading to trapping at the longest segment.

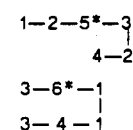


Figure 10. Schematic representation of downhill EET in a chain of segments of various conjugation length, represented by the number of conjugated units. The emitting segment is indicated by an asterisk.

they also observe differences in the spectral distribution of the emission of two polarized components.

To explain our result, it is assumed that all molecules that orientate parallel to the stretching direction undergo more conformational changes than the less oriented fraction, which is preferentially monitored by I_{HVV} . In a more elongated overall conformation of the macromolecule, the preferred pathway of EET is along the chain. With a random sequence of conjugated segments of various length this implies that the excitation can be immobilized at energetically higher segments from which EET is improbable. The process is illustrated as case B in a simplified way in Figure 10.

The influence of the coil conformation on EET will be further substantiated by measurements in a different polymer matrix and by time-resolved fluorescence.

Acknowledgment. Financial support by the Fonds der Chemischen Industrie and by the Deutsche Forschungsgemeinschaft is gratefully acknowledged. The authors thank A. Greiner, Marburg, Germany, who sup-

plied poly(*p*-phenylphenylenevinylene), and H. Meier, Mainz, Germany, who supplied 1,4-distyrylbenzene.

References and Notes

- (1) Friend, R. H.; Bradley, D. D. C.; Townsend, P. D. *J. Phys. D: Appl. Phys.* **1987**, *20*, 1367.
- (2) Bradley, D. D. C.; Friend, R. H. *J. Mol. Electron.* **1989**, *5*, 19.
- (3) Rauscher, U.; Schütz, L.; Greiner, A.; Bäessler, H. *J. Phys.: Condens. Matter* **1989**, *1*, 9751.
- (4) Furukawa, M.; Mizuno, K.; Matsui, A.; Rughooputh, S. D. D. V.; Walker, W. C. *J. Phys. Soc. Jpn.* **1989**, *58*, 2976.
- (5) Rauscher, U.; Bäessler, H.; Bradley, D. D. C.; Hennecke, M. *Phys. Rev. B* **1990**, *42*, 9830.
- (6) Campbell, D. K. *Mol. Cryst. Liq. Cryst.* **1990**, *189*, 65.
- (7) Bradley, D. D. C.; Friend, R. H.; Wong, K. S.; Hayes, W.; Lindenberger, H.; Roth, S. *Springer Ser. Solid State Sci.* **1987**, *76*, 107.
- (8) Hörhold, H. H.; Helbig, M. *Makromol. Chem., Macromol. Symp.* **1987**, *12*, 229.
- (9) Drehfahl, G.; Kühmatdt, R.; Oswald, H.; Hörhold, H. H. *Makromol. Chem.* **1970**, *131*, 89.
- (10) Obrzut, J.; Karasz, F. E. *J. Chem. Phys.* **1987**, *87*, 2349.
- (11) Oberski, J. M.; Greiner, A.; Bäessler, H. *Chem. Phys. Lett.* **1991**, *184*, 391.
- (12) Mahrt, R.; Yang, J.; Greiner, A.; Bäessler, H. *Makromol. Chem., Rapid Commun.* **1990**, *11*, 415.
- (13) Stenger-Smith, J. D.; Lenz, R. W.; Wegner, G. *Polymer* **1989**, *30*, 1048.
- (14) Wong, K. S.; Bradley, D. D. C.; Hayes, W.; Ryan, J. F.; Friend, R. H.; Lindenberger, H.; Roth, S. *J. Phys. C: Solid State Phys.* **1987**, *20*, L187.
- (15) Tokito, S.; Saito, S. *Makromol. Chem., Rapid Commun.* **1986**, *7*, 557.
- (16) Hennecke, M. *Synth. Met.* **1991**, *41*, 1281.
- (17) Fredrickson, G. H.; Andersen, H. C.; Frank, C. W. *J. Polym. Sci., Polym. Phys. Ed.* **1985**, *23*, 591.
- (18) Peterson, K. A.; Fayer, M. D. *J. Chem. Phys.* **1986**, *85*, 4702.
- (19) Hennecke, M.; Kauffmann, H. F. *Chem. Phys.* **1991**, *158*, 391.
- (20) Peterson, K. A.; Zimmt, M. B.; Fayer, D.; Jeng, Y. H.; Frank, C. W. *Macromolecules* **1989**, *22*, 874.
- (21) Fredrickson, G. H.; Andersen, H. C.; Frank, C. W. *Macromolecules* **1983**, *16*, 1456.
- (22) Andrews, D. L.; Juzeliūnas, G. *J. Chem. Phys.* **1991**, *95*, 5513.
- (23) Stein, A. D.; Peterson, K. A.; Fayer, M. D. *J. Chem. Phys.* **1990**, *92*, 5622.
- (24) Sienicki, K.; Itagaki, H.; Mattice, W. L. *J. Chem. Phys.* **1989**, *91*, 4515.
- (25) Knox, R. S. *Physica* **1968**, *39*, 361.
- (26) Knoester, J.; Van Himbergen, J. E. *J. Chem. Phys.* **1986**, *84*, 2990.
- (27) Weber, G. In *Fluorescence and Phosphorescence Analysis*; Hercules, D. M., Ed.; Interscience Publishers: New York, 1966; p 217.
- (28) Weber, G. *Trans. Faraday Soc.* **1954**, *50*, 552.
- (29) Michl, J.; Thulstrup, E. W. *Spectroscopy with Polarized Light*; VCH Publishers: New York, 1986.
- (30) Nobbs, J. H.; Bower, D. I.; Ward, I. M.; Patterson, D. *Polymer* **1974**, *15*, 287.
- (31) Nobbs, J. H.; Ward, I. M. In *Polymer Photophysics*; Phillips, D., Ed.; Chapman and Hall: London, 1985; Chapter 4.
- (32) Kimura, I.; Kagiya, M.; Nomura, S.; Kawai, H. *J. Polym. Sci., Polym. Phys. Ed.* **1969**, *7*, 709.
- (33) Hennecke, M.; Fuhrmann, J. *Colloid Polym. Sci.* **1980**, *258*, 219.
- (34) Schenk, R.; Gregorius, H.; Meerholz, K.; Heinze, J.; Müllen, K. *J. Am. Chem. Soc.* **1991**, *113*, 2634.
- (35) Martelock, H.; Greiner, A.; Heitz, W. *Makromol. Chem.* **1991**, *192*, 967.
- (36) Desper, C. R.; Kimura, I. *J. Appl. Phys.* **1967**, *38*, 4225.
- (37) Sandros, K.; Sundahl, M.; Wennerström, O.; Norinder, U. *J. Am. Chem. Soc.* **1990**, *112*, 3082.
- (38) Oelkrug, D.; Rempfer, K.; Prass, E.; Meier, H. *Z. Naturforsch.* **1988**, *43A*, 583.
- (39) Castel, N.; Fischer, E.; Bartocci, G.; Masetti, F.; Mazzucato, U. *J. Chem. Soc., Perkin Trans. 2* **1985**, 1969.
- (40) Dale, R. E.; Bauer, R. K. *Acta Phys. Pol.* **1971**, *A40*, 853.
- (41) Weber, G. *Biochem. J.* **1960**, *75*, 335.
- (42) Weber, G. *J. Opt. Soc. Am.* **1956**, *46*, 962.
- (43) Greiner, A., personal communication.
- (44) Shinitzky, M.; Dianoux, A. C.; Gitler, C.; Weber, G. *Biochemistry* **1971**, *10*, 2106.
- (45) Kowski, A.; Kojoro, Z.; Bojarski, P.; Lichacz, J. *Z. Naturforsch.* **1990**, *45A*, 1357.
- (46) Weber, G.; Anderson, S. R. *Biochemistry* **1969**, *8*, 361.
- (47) Fuhrmann, J.; Hennecke, M. *Makromol. Chem., Macromol. Symp.* **1989**, *26*, 209.
- (48) Hennecke, M. *J. Polym. Sci., Polym. Phys. Ed.* **1986**, *24*, 111.
- (49) Hagler, T. W.; Pakbaz, K.; Moulton, J.; Wudl, F.; Smith, P.; Heeger, A. J. *Polym. Commun.* **1991**, *32*, 339.
- (50) Hagler, T. W.; Pakbaz, K.; Voss, K. F.; Heeger, A. J. *Phys. Rev. B* **1991**, *44*, 8652.